Thesis Report

On

EXPERIMENTAL AND NUMERICAL ANALYSIS OF TENSILE TEST

Submitted in the partial fulfillment of requirement for the award of the degree of

Master of Engineering

IN

CAD/CAM and ROBOTICS

Submitted by

GURPREET KAUR
Roll No. : 8048126

Under the guidance of

Mr. J.S. SAINI
Lecturer
T.I.E.T, Patiala

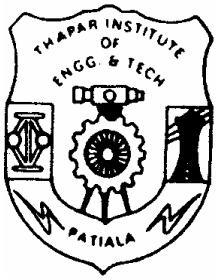

Department of Mechanical Engineering
THAPAR INSTITUTE OF ENGINEERING AND TECHNOLOGY
(DEEMED UNIVERSITY)
PATIALA (PUNJAB)-147004

CERTIFICATE

This is to certify that the Thesis report entitled, **"EXPERIMENTAL AND NUMERICAL ANALYSIS OF TENSILE TEST"** submitted by **Ms. GURPREET KAUR** in the partial fulfillment of the requirement for the award of the degree of **Master of Engineering in Mechanical (CAD/CAM and ROBOTICS) Engineering** to **Thapar Institute of Engineering and Technology (Deemed University), Patiala,** is a record of candidate's own work carried out by her under my supervision and guidance. The matter embodied in this report has not been submitted in part or full to any other university or institute for the award of any degree.

(Mr. J.S.SAINI)
Lecturer, Mechanical Engineering Department.
Thapar Institute of Engg. &Technology,Patiala

Countersigned by:

Dr. S.K. MOHAPATRA
Prof. & Head, MED.
THAPAR INSTITUTE OF ENGG. &TECH.
PATIALA-147004(PUNJAB)

Dr. T.P. SINGH
Dean, Academic Affairs
THAPAR INSTITUTE OF ENGG. &TECH.
PATIALA-147004(PUNJAB)

Dated:

Acknowledgement

I express my sincere gratitude to my guide**, Mr. J.S.SAINI** Lecturer, Mechanical Engg. Department at Thapar Institute of Engineering & Technology, for his valuable guidance, proper advice, painstaking and constant encouragement during the course or my work on this seminar.

I also feel very much obliged to **Dr. S.K MOHAPATRA,** Professor & Head, Department of Mechanical Engg. for his encouragement and inspiration for execution of the seminar work.

I am deeply indebted to my parents for their inspiration and ever encouraging moral support, which enabled me to pursue my studies.

I am also very thankful to the entire faculty and staff members of Mechanical engineering Department for their direct–indirect help and cooperation.

Dated:

GURPREET KAUR

(ROLL NO. 8048126)

ABSTRACT

Tensile test is an important standard engineering procedure to characterize properties related to mechanical behaviour of materials. To properly describe the response of the material during the actual loading conditions, the variation in geometry of the specimen has to be considered. Although the behaviour of the material in elastic limit is of considerable importance but the knowledge beyond elastic limit is also relevant since plastic effects with large deformation takes place in number of manufacturing processes.

The mechanical behaviour of Corten Steel, used in manufacturing of railway coaches are important properties used in the crash analysis of the component. Finite Element Method being a widely used tool for analysis due to revolution in computer field is used for the analysis of the components.

The present work describes the behavior of Corten Steel sheet specimens in plastic range. Finite element method was employed for the analysis of tensile test.

LIST OF FIGURES

CHAPTER 1

CHAPTER 3

CHAPTER 4

LIST OF TABLES

CHAPTER 4

CHAPTER 1

INTRODUCTION

The present work deals with the experimental and numerical analysis of tensile test on Corten Steel material which is used in rail coaches. Brief overviews of the related terms are given in this chapter.

To characterize some relevant elastic and plastic variables related to the mechanical behaviour of materials, the Tensile Test is a useful important standard engineering procedure. Due to the non-uniform stress and strain distributions existing at the neck for high levels of axial deformation, it has been long recognized that significant changes in the geometric configuration of the specimen have to be considered in order to properly describe the material response during the whole deformation process up to the fracture stage.

Although in many engineering applications the design of structural parts is restricted to the elastic response of the material involved, the knowledge of their behaviour beyond the elastic limit is relevant since plastic effects with large deformations take place in the manufacturing processes such as metal forming example: forging, drawing, extrusion, rolling, deep drawing, magnetic pulse forming, and tube enlarging and bulging. Other important applications of elastoplastic models for: Crashworthiness, impact problems, inelastic buckling of thin-walled structures, super plastic forming etc.

1.1 TENSILE TEST

The engineering tensile test also known as tension test is widely used to provide basic design information on the strength of material and as an acceptance test for the specification of the materials. Tensile tests are simple, relatively inexpensive, and fully standardized. By pulling on something, it can be very quickly determined how the material will react to forces being applied in tension. As the material is being pulled, its strength along with how much it will elongate can be find out. A lot about a substance can be learned from tensile testing. As the machine continues to pull on the material until

it breaks, a good, complete tensile profile is obtained. A curve will result showing how it reacted to the forces being applied. In the tensile test a specimen is subjected to a continually increasing uniaxial tensile force while simultaneous observations are made of the elongation of the specimen. Fig 1.1 shows a typical stress-strain curve for a metal.

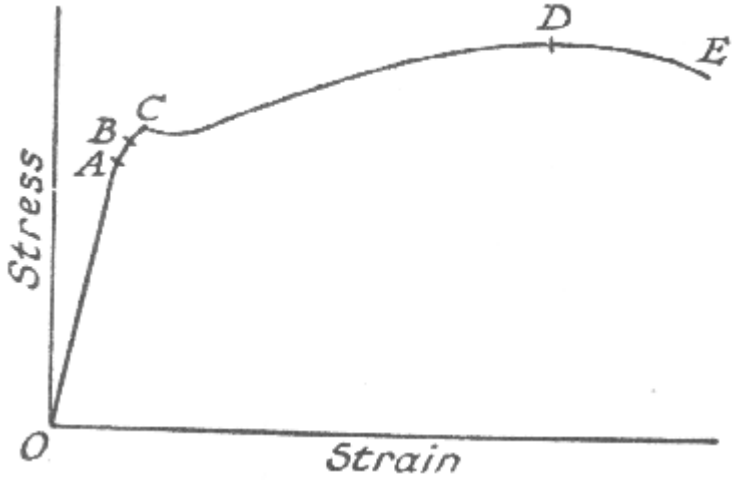

Fig 1.1 Typical Stress-Strain Curve

For the very small strains involved in the early part of the test, the elongation of a measured length is recorded by an extensometer. The load is increased gradually, and at first the elongation and hence the strain, is proportional to the load and hence to the stress. This relation (*Hooke's Law*) holds up to a value of the stress known as the limit of proportionality(*Point A*).Hooke's law ceases to be obeyed this point, although the material may still be in the "elastic" state. The *point B* shows the *elastic limit*. If the material is stressed beyond this point, some plastic deformation will occur. The next important occurrence is the yield *point C*, at which the metal shows an appreciable strain even without further increase in load. For materials showing no definite yield, a *proof stress* is used to determine the onset of plastic strain.

After yielding has taken place, further straining can only be achieved by increasing the load, the stress-strain curve continuing to rise up to the *point D*. The strain in the region from C to D is 100 times the strain in the system from O to C, and is partly elastic (i.e. recoverable), but mainly plastic (i.e. permanent strain). At this stage (D) the bar begins to form a local "neck", the load falling off from the maximum until fracture at E. The proportional limit is the stress at which the stress-strain curve deviates from linearity. The slope of the stress-strain curve is the modulus of elasticity. Plastic

deformation begins when the elastic limit is exceeded. As the plastic deformation of the specimen increases, the metal becomes stronger so that the load required to extend the specimen increases with further straining. Eventually the load reaches a maximum value. The maximum load divided by the original area of the specimen is the ultimate tensile strength. For a ductile metal the diameter of the specimen begins to decrease rapidly beyond maximum load, so that the load required to continue deformation drops off until the specimen fractures. Since the average stress is based on original area of the specimen, it also decreases from maximum load to fracture.

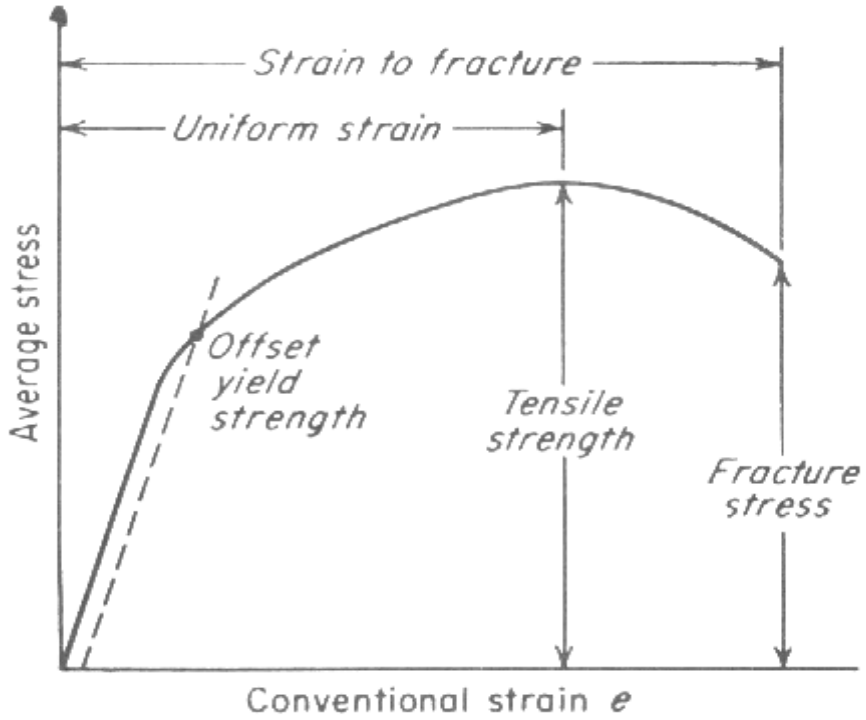

Fig 1.2 The Engineering Stress-Strain Curve

An engineering stress-strain curve is constructed from the load-elongation measurements (fig.1.2). The stress used in this stress-strain curve is the average longitudinal stress in the tensile specimen. It is obtained by dividing the load by the original area of the cross-section of the specimen.

$$S = P/A_0 \tag{1.1}$$

The strain used for the engineering stress-strain curve is the average linear strain, which is obtained by dividing the elongation of the gauge length of the specimen, δ, by its original length.

$$e = \frac{\delta}{L_0} = \frac{\Delta L}{L} = \frac{L - L_0}{L_0} \tag{1.2}$$

The shape and magnitude of the stress-strain curve of a metal will depend upon its composition, heat treatment, prior history of plastic deformation, and the strain rate, temperature, and state of stress imposed during the testing. The parameters which are used to describe the stress-strain curve of a metal are the *tensile strength, yield strength* or *yield point, percentage elongation* and *reduction of area.* The first two are strength parameters; the last two indicate ductility.

In the elastic range, strain is measured by an "extensometer" attached to the gauge length. In the elastic region stress is linear proportional to strain. When the load exceeds a value corresponding to the yield strength, the specimen undergoes plastic deformation. It is permanently deformed if the load is released to zero. The stress to produce continued plastic deformation increases with increasing plastic strain i.e. the metal strain-hardens. The volume of the specimen remains constant during plastic deformation,

$$AL = A_0 L_0 \tag{1.3}$$

and as specimen elongates, it decreases uniformly along the gauge length in cross-sectional area. Initially the strain hardening more than compensates for this decrease in area and the engineering stress continues to rise with increasing strain. Eventually, a point is reached where the decrease in specimen cross-sectional area is greater than the increase in deformation load arising from strain hardening. This condition will be reached first at some point in the specimen that is slightly weaker than the rest. All further plastic deformation is concentrated in this region, and the specimen begins to neck or thin down locally .Because the cross-sectional area now is decreasing far more rapidly than the deformation load is increased by strain hardening, the actual load required to deform the specimen falls off and the engineering stress likewise continues to decrease until fracture occurs. Many varieties of fractures can occur during the processing of metals and their use in different types of service. One of them is the Ductile Fracture.

1.1.1 DUCTILE FRACTURE

Ductile fracture is been defined as fracture occurring with appreciable gross deformation. Ductile fracture in tension is usually preceded by a localized reduction in diameter called necking. Very ductile metals may actually draw down to a line or a point before separation. This kind of failure is usually called rupture.

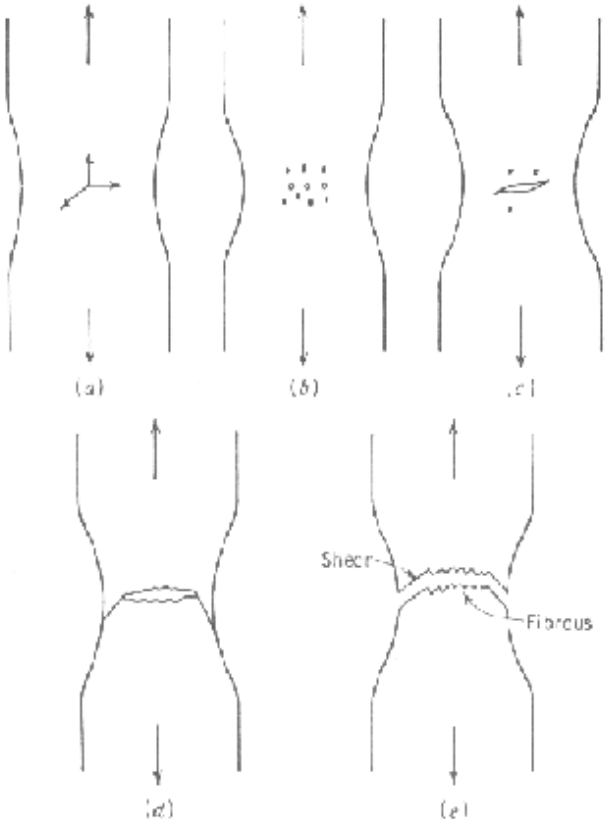

Fig 1.3 Stages in the formation of a cup-and-cone fracture.

The stages in the development of a ductile “cup-and-cone” fracture are illustrated in fig. 1.3.Necking begins at the point of plastic instability where the increase in strength due to strain hardening fails to compensate for the decrease in cross-sectional area (fig. 1.3a).This occurs at the maximum load or at a true strain equal to the strain-hardening coefficient. The formation of a neck introduces a triaxial state of stress in the region. A

hydrostatic component of tension acts along the axis of the specimen at the center of the necked region.

Many fine cavities form in this region (Fig.1.3b), and under continued straining these grow and coalesce into a central crack (Fig.1.3c).This crack grows in a direction perpendicular to the axis of the specimen until it approaches the surface of the specimen. It then propagates along localized shear planes at roughly 45^0 to the axis to form the "cone" part of the fracture (Fig.1.3d).

Universal Testing Machine is used to conduct the tensile test.Two general types of machines are used in tension testing :(1) load controlled machine and (2) displacement controlled machines.

1.1.2 UNIVERSAL TESTING MACHINE

The more recently developed servo hydraulic testing machines provide both load or displacement control. These versatile machines are well adapted to computer control. With modern computer control it is possible to conduct tests based on the control of calculated variables such as true strain or stress intensity factor. Fig1.4 shows a picture of UTM.

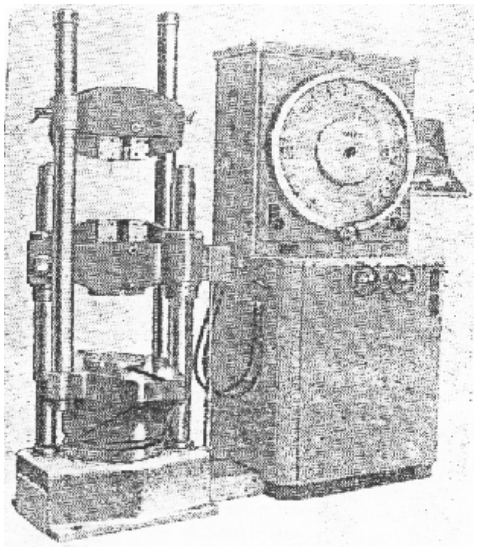

Fig1.4 Universal Testing Machine

The top crosshead can be adjusted to three positions for extended tension tests (the left hand side of the machine). There are two main hand wheel controls, one for

applying and the other for releasing the load. The loading valve is so designed that at any setting, needed for applying incremental loads, for applying the loads quickly, for holding the loads steady and for removing the loads. An autographic recorder can be used to plot the stress-strain curve during the test itself

Specimens were attached to a movable grip and to a fixed side-gripping device. A parallel spring was made of four thin plates to serve as the straight guide mechanism for the movable grip. The movable grip and the straight guide mechanism were lifted over the base of the tensile testing machine so that they were not affected by friction which would otherwise seriously impair the accuracy of the tensile tests. Load was applied by pulling (using a precision translation stage driven by a d.c. motor) one end of steel belt, the other end, of which, was connected to the movable grip. A load cell with a rated capacity was used to measure the load, which was the sum of the loads applied to the specimen and the parallel spring. The load applied to the specimen was calculated by subtracting the load applied to the parallel spring, calculated from the characteristics of the parallel spring measure in advance, from the measure load.The elongation was determined by measuring the relative displacement of the two gauge marks on the specimen.

The characteristics of the testing machine can have a strong influence on the shape of the stress-strain curve and the fracture behaviour .a rigid testing machine with a spring constant is known as a hard machine. A screw-driven mechanical machine tends to be hard machines, while hydraulically driven testing machines are soft machines. A hard testing machine will reproduce faithfully the upper and lower yield point, but in a soft machine these will be smeared out and only the extension at constant load will be recorded.

1.2 FINITE ELEMENT METHOD

The term *finite element* was first coined and used by Clough in 1960. Since then it has become a powerful tool for the numerical solution of a wide range of engineering problems. Applications range from deformation and stress analysis of automotive, aircraft, building and bridge structures to field analysis of heat flux, fluid flows, magnetic flow, seepage, and other flow problems.

Earlier the design of a component was based on experimental data and manual calculations which was a time consuming process and yield lesser degree of safety and optimization of the product.Moreover,the design so produced is accepted after a series of prototype test which requires a huge amount of money and time involvement.So,With the advances in computer technology and CAD systems, complex models can be modeled with relative ease and also several tests can be made prior to going for the final prototype. As the technology is improving day by day, their are some very good software's in the market of *finite element analysis*. So, finite element analysis is very much useful in designing and testing of various components and materials, which are constantly under different types of loads and under different conditions such as bending, torsion, tension or compression. That's why nowadays FEM is so popular. Moreover, FEM is based on matrices and they require less time and memory of computers.

In this method of analysis, a complex region defining a continuum is discretized into simple geometric shapes called finite elements. The material properties and the governing relationships are considered over these elements and expressed in terms of unknown values at element corners. After this an assembly process, duly considering the loading and constraints gives a set of equations, which on solving gives us the approximate behavior of the continuum.

A finite element analysis involves three stages of activity: *preprocessing, processing and post processing.* Preprocessing involves the preparation of data, such as nodal coordinates, connectivity, boundary conditions, and loading and material information. The processing stage involves mesh generation, stiffness generation, stiffness modification, and solution of equations, resulting in the evaluation of nodal variables. Other derived quantities, such as gradients or stresses may be evaluated in this stage. The post processing stage with the preparation of results. Typically, the deformed configuration, mode shapes, temperature, and stress distribution are computed and displayed at this stage. A complete finite element analysis is a logical interaction of the three stages.

1.2.1 APPLICATIONS OF FINITE ELEMENT ANALYSIS

The most utilization of FEM is in finding stresses and strains caused by loading conditions on a part. Other uses of FEM include:

- Static stress-strain problems
- Non-linear problems
- Heat transfer problems
- Modal analysis
- Dynamic analysis
- Electricity and magnetism problems
- Flow problems
- Acoustic problems and other engineering problems in various fields

Now considering the Non-linear type of problem, we first have to get an insight of what are these problems and how these are solved.

1.3 NONLINEAR PROBLEM

Some everyday situations are nonlinear, and you probably don't even recognize them: pressing your finger against a balloon to see a dimple; flexing a paper clip back and forth; crushing an aluminum can so that it buckles; and hitting a pothole in the road. These cases all exhibit large deformations, and sometimes, inelastic material behaviour. The three major types of nonlinearities are:

- **Material Nonlinearity** (plasticity, creep, viscoelasticity)
- **Geometric Nonlinearity** (large deformations, large strains, snap-through buckling)
- **Boundary Nonlinearity** (opening/closing of gaps, contact, follower force).

Of course, there can be combinations of any of these. To find evidence of possible nonlinear behavior, look for: permanent deformations and any gross changes in geometry, cracks, necking, thinning, distortions in open section beams, crippling, buckling, stress values which exceed the elastic limits of the materials, evidence of local yielding, shear bands, and temperatures above 30% of the melting temperature. In these cases, the stress is no longer proportional to the strain. The nonlinear problems are inherently more complex to analyze than linear problems. And, the "principle of

superposition" (which states that the resultant deflection, stress, or strain in a system due to several forces is the algebraic sum of their effects when separately applied) no longer applies. Finite element analysis is an approximate analysis method which is only as accurate as:

- *The quality of the model*
- *The material properties used (and their assumptions)*
- *Representation of the loads and boundary conditions*
- *The solution algorithm.*

In nonlinear FEA, the following relationships (which are assumed to be linear in linear FEA) may be violated:

1. The strain is no longer small.

Most metallic materials are no longer useful when the strain exceeds one or two percent. However, some materials, notably rubbers, elastomers, and plastics, can be strained to hundreds of a percent and will therefore require finite (large) strain analysis.

2. The strain-displacement relationship is no longer linear.

This is true if the rotations become large even though the strains are still small. The changes in the deformed shape can no longer be ignored. The physics of buckling, rubber analysis, metal forming, among others, requires that either a quadratic relationship exits between the strain and displacement (Green-Strain) or a logarithmic relationship exists. Engineering stress is no longer appropriate because of geometric changes and the true stress or Cauchy stress should be used.

3. The stress-strain law may become nonlinear.

Even within the useful stress range of the material. This behavior is typical of most metals, rubbers and elastomers, and certain composite materials whose properties are unequal in tension and compression.

4. The original equilibrium equations (relating stress to loads) may have to be updated.

Due to the geometrical changes in the shape of the structure. These relations mean that, in nonlinear FEA, the load is no longer proportional to the displacement, that is, $F \neq Ku$.

When stresses go beyond the linear elastic range, material behavior can be broadly divided into two classes:

- **Time-independent behavior** (plasticity-applicable to most ductile metals; nonlinear elasticity-applicable to rubber, elastomers)
- **Time-dependent behavior** (creep, viscoplasticity-applicable to high-temperature applications, concrete;viscoelasticity-applicable to elastomers, glass, plastics).

An elasticplastic material may be defined as a material, which, upon reaching a certain stress state, undergoes deformation, which is irreversible. This results in a behavior, which is path-dependent. A basic assumption in elastic-plastic analysis is that deformation can be divided into an elastic part and an in elastic (plastic) part.

- **Yield Conditions** The *yield stress* is a measured value that separates the elastic and inelastic behavior of a material. Its magnitude is usually obtained from a uniaxial test. However, stresses in a structure are multiaxial, and a measure of yielding in a multiaxial state of stress is called the "yield condition" or "yield criterion."
- **Work Hardening Rules** In a uniaxial test, the work hardening slope is defined as the slope of the stress-plastic strain curve. It relates the incremental stress to incremental plastic strain in the inelastic region and dictates the conditions of subsequent yielding. The *isotropic* hardening rule assumes that the center of the yield surface remains stationary in the stress space, but the size (radius) of the yield surface expands due to strain hardening. It is considered suitable for problems in which the plastic straining far exceeds the incipient yield state.
- **Large Deformations** In implicit analysis, the relationship between incremental load ΔF and displacement Δu is called a tangent stiffness KT. This stiffness has three components: the material stiffness, the initial stress stiffness, and the geometric stiffness. The material stiffness may be the same elastic stiffness as that used in linear FEA. The second term represents the resistance to load caused by realigning the current internal stresses when displacements occur. The third term

represents the additional stiffness due to the nonlinear strain-displacement relationship.

Before, the formulation of nonlinear finite element problem, it is useful to familiarize ourselves with the theory of plasticity.

1.4 PLASTICITY THEORY

Plasticity refers to the non-recoverable deformation and non-unique stress paths in contrast to nonlinear elasticity, where the entire load deflection path is unique and the strains are recovered on load removal. The mathematical model theory of plasticity is of phenomenological nature on the macroscopic scale, and the objective of the theory is to provide a theoretical description of the relationship between stress and strain for a material that exhibits an elasto-plastic response. The plastic behaviour is characterized by irreversibility of stress paths and the development of permanent (i.e. non-recoverable) deformation (or strain), known as yielding (or plastic flow).

If uniaxial behavior of a material is considered, a non-linear stress-strain relationship on loading alone does not determine if nonlinear elastic or plastic behaviour is exhibited. Unloading part of the curve determines if it is elastic or plastic (fig 1.5(a) and (b)); the elastic material follows the same path in loading and unloading ,while the plastic material shows a history-dependent part unloading.

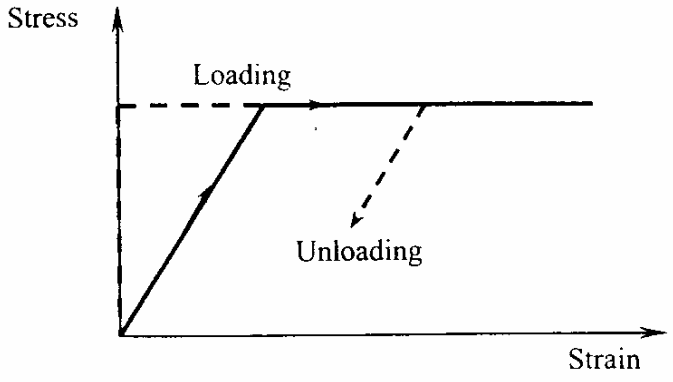

(a)

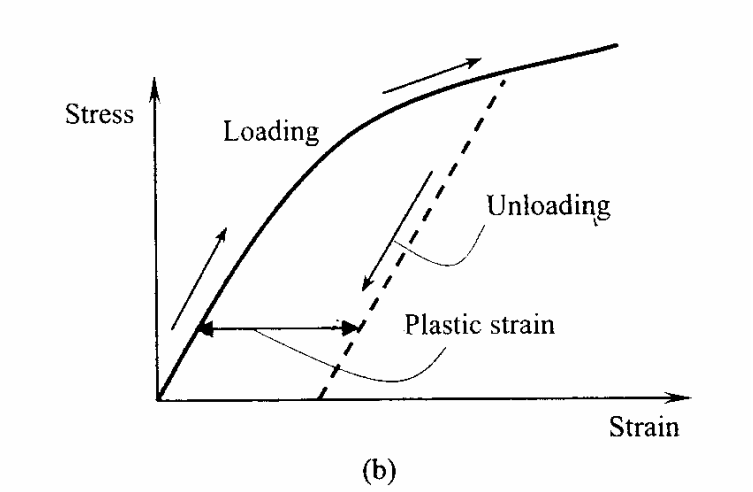

Fig 1.5 stress-strain behavior of (a) ideal plasticity, and (b) strain-hardening plasticity

The theory of plasticity deals with an analytical description of the stress-strain relations of a deformed body after a part or all of the body has yielded. The stress-strain relation must contain:

1. The elastic stress-strain relations.
2. The stress condition (or yield criterion) which indicates onset of yielding.
3. The stress-strain or stress-strain increment relations after the onset of plastic flow.

The plastic stress-strain relations will include work-hardening in certain cases, though it is not possible to take work-hardening fully into account in general case. The above relations are based on experiments carried out under uniform stress conditions. Their validity when applied to non uniform stress systems must be checked by experiment. Again, since the actual stress-strain relations vary with the speed of deformation and the ambient temperature, it is very important to obtain the experimental stress-strain curve under conditions similar to those existing in the system under consideration. In order to obtain a solution to a deformation problem, it is necessary to idealize the stress-strain relation.

1.4.1 IDEAL PLASTICITY

Many materials exhibit an ideal plastic (or elastic-perfectly –plastic) behavior, as shown in fig 1.5(a). In this case, there exists a limiting stress, called yield stress, denoted by σ_Y, at which the strain are indeterminate. For all stresses below the yield stress, a linear (or non-linear) stress-strain relation is assumed:

$\sigma_{ij} < \sigma_Y$ Linear elastic behavior

$\sigma_{ij} \geq \sigma_Y$ Plastic deformation (not recoverable)

1.4.2 STRAIN HARDENING PLASTICITY

A Hardening Plastic Material Model provides a refinement of the ideal plastic material model. In this model, it is assumed that the yield stress depends on some parameter κ (e.g. plastic strain ε^p), called the hardening parameter. The general yield criterion is expressed in the form

$$F(\sigma_{ij}, \kappa) = 0 \tag{1.4}$$

This yield criterion can be viewed as a surface in the stress space, with the position of the surface dependent on the instantaneous value of the hardening parameter κ. Since any yield criterion should be independent of the orientation of the coordinate system used, *F* must be a function of the stress invariants only. Experimental observations indicate that plastic deformation in metals is independent of hydrostatic pressure. Therefore, *F* must be a function of the stress invariants of the deviatoric stress tensor σ':

$$F(J_2', J_3', \kappa) = 0, J_2' = \frac{1}{2}\sigma_{ij}'\sigma_{ij}', J_3' = \frac{1}{3}\sigma_{ij}'\sigma_{jk}'\sigma_{ki}' \tag{1.5}$$

Two of the most commonly used criteria are given next.

The Tresca yield criterion

$$F = 2\bar{\sigma}\cos\theta - Y(\kappa) = 0, \bar{\sigma} = \sqrt{J_2'} \tag{1.6}$$

The Huber-von Mises yield criterion

$$F = \sqrt{3J_2'} - Y(\kappa) = 0 \tag{1.7}$$

where *Y* is the yield stress from uniaxial tests, θ is the angle between the line of pure shear and the principal stress σ_1, and $\bar{\sigma} = \sqrt{J_2'}$ is called the effective stress.

After initial yielding, the stress level at which further plastic deformation occurs may be dependent on the current degree of plastic straining, known as strain hardening. Thus, the yield surface will vary (i.e. expand) at each stage of plastic deformation .when the yield surface is independent of the degree of plasticity, the material is said to be ideally (or perfectly) plastic.

CHAPTER 2

LITERATURE REVIEW

This chapter deals with the review of work done related to topic. Firstly the review is on the tensile test which is a standardized mechanical test which is widely used to reveal the mechanical behaviour of lot of materials. It is an important test to ensure that the particular material can withstand the given load and given conditions. Then the concentration shifts on the review of finite element method and elastoplastic analysis. To study and analyze a material, Finite Element Method analysis of components is an important tool which is widely used.

2.1 LITERATURE REVIEW

Simo and Armero [1] have presented a class of 'assumed strain' mixed finite element methods for fully non-linear problems in solid mechanics is presented which, when restricted to geometrically linear problems, encompasses the classical method of incompatible modes as a particular case. The method relies crucially on a local multiplicative decomposition of the deformation gradient into a conforming and enhanced part, formulated in the context of a three-field variational formulation. The resulting class of mixed methods provides a possible extension to the non-linear regime of well-known incompatible mode formulations. The good performance of the proposed methodology is illustrated in a number of simulations including 2-D, 3-D and axisymmetric finite deformation problems in elasticity and elastoplasticity.

Morestin *et. al* [2] developed a logic which computes the deformation of steel sheet in press forming after spring back. Work hardening of steel involves modifications of the elastic properties of the material, e.g. an increase in its yield stress. It can also be the cause of an appreciable decrease in the Young modulus. However, this property diminishes as the plastic strain increases. The purpose of the experiments with a

microcomputer-controlled tensile test machine is to indicate that the diminution can reach more than 10%, of the initial value after only 5% plastic strain. In spite of this fact, a lot of elastic-plastic software does not take into account the decrease in the Young modulus with plastification even though it may lead to obvious differences among results. So, as an application they developed the software. The software takes into account the decrease in the Young modulus and its results are very close to experimental values. They noticed a recovery of the Young modulus of plastified specimens after few days, but not for all steels tested. The Young modulus vs. plastic strain allows a better numerical analysis of an elastic plastic phenomenon such as spring back. The introduction of the behaviour in other software simulations of metal forming seems equally as necessary as the correct determination of the general work-hardening parameters of the material. The recovery phenomenon of the Young modulus after plastification for materials such as XC38, A33 and Bronze-aluminium is little known at this time. Its influence on the shape of the specimen remains to be shown. The recovery shows as well that, for the metals already cited, the apparent Young modulus cannot be used as a permanent damage indicator for plastic strains lower than 15%.

Ling [3] presented a weighted-average method for determining uniaxial, true tensile stress vs. strain relation for strip shaped samples after necking .The method requires identification of a lower and an upper bound for the true stress-strain function after necking and expresses the true stress-strain relation as the weighted average of these two bounds. The weight factor is determined iteratively by a finite element model until best agreement between calculated and experimental load extension curves is achieved. The method was applied to various alloys.

Albertini *et. al* [4] have dealt with modelling of experimental data concerning tension and shear of AISI 316H for low, medium and high strain rates for large viscoplastic strains in this paper. Main results are: a) linearity between equivalent plastic strain rate and equivalent stress rate leading to an endochronic understanding of time in evolution equations and b) Chaboche model generalized to include large strains is compared with Rice-Ziegler model with tensor representation.

Mariani *et. al* [5] have presented and simulated quasi-static ductile fracture processes d within the framework of the finite element method by means of the Gurson–Tvergaard isotropic constitutive model for progressively cavitating elastoplastic solids. The progressive degradation of the material strength properties in the fracture process zone due to micro-void growth to coalescence is modeled through the computational cell concept. To identify these model parameters the inverse problem is solved via the extended Kalman filter for nonlinear systems coupled to a numerical methodology for the sensitivity analysis. In part I of this work the theory of Kalman filtering and sensitivity analysis is presented. First results concerning the identification of the Tvergaard parameters for a whole crack growth in single edge notched bend specimens made of a pressure vessel steel are presented. In order to enhance the convergence towards the final solution of the identification procedure, during the tests measurements are made of the displacements of points located in the central portion of the notched specimens, where model parameters highly affect the system state variables. In part II of this work a numerical validation of the proposed procedure in terms of uniqueness of the final identified solution, requirements of accuracy for the Bayesian initialization of the model parameters and sensitivity to the experimental measurement errors will be presented and discussed.

Celentano [6] presented a large strain thermoviscoplastic formulation for the analysis of the solidification process of spheroidal graphite (S.G) cast iron in a green sand mould. This formulation includes two different non-associate constitutive models in order to describe the thermo mechanical behaviour of each of such materials during the whole process. The performance of these models is evaluated in the analysis of a solidification test.

Govaert *et. al* [7] investigated the process of blanking of a ferritic stainless steel in various blanking geometries with respect to rate-dependence by employing an elasto-viscoplastic constitutive model in combination with the postulated fracture criterion for ferritic stainless steel .The approach was based on the finite element method, employing a rate-independent elasto-plastic constitutive model combined with a fracture criterion

which accounts for the complete loading history. Numerical predictions were compared to experimental data over a large range of process speeds. The rate-dependence of the process force is significant and accurately captured by the numerical simulations at speeds ranging from 0.001 to 10 mm/s. Both experiments and numerical simulations show no influence of punch velocity on fracture initiation. Up to blanking velocities of 10 mm/s which was within the range of nearly every industrial application. The blanking speed has no influence on the punch displacement at ductile fracture initiation for X30Cr13. It was an important conclusion, because it has shown that blanking processes with punch velocities smaller than 10 mm/s can be described by the elasto-plastic constitutive model using Von Mises plasticity, when ductile fracture initiation was considered. When process forces were considered, the effect of the strain rate was small but noticeable. Therefore, if the correct prediction of the blanking force as a function of the strain rate is not an issue, the constitutive model using Von Mises plasticity will suffice.

Gozzi *et. al* [8] have presented a constitutive model proposed for stainless steel. The model is a two surface model utilizing the concept of fuzzy sets. An experimental investigation has been performed on two different stainless steel grades as a reference to the model. The tests were performed with a procedure containing load reversal. Each specimen was initially loaded in one direction of the principal stress plane followed by unloading and subsequent loading in a new direction. The model is relatively simple but still depicts the effects of observed phenomena such as the Bauschinger effect. Hence the qualitative response to subsequent loadings can be described with the model. The proposed model has been implemented into the finite element package ABAQUS. Comparisons between test results and the response predicted utilizing the model are presented in this paper.

Kang *et. al* [9] proposed two new kinds of specimens, one is a multi-stepped specimen that can be traced to the three stepped specimen, and the other is a tapered specimen which decreases the complexity of the multi-stepped specimen in manufacture and studied their behavior. In order to study metal behavior, it is very important to

establish a method to create a large strain hardening curve based on the normal mechanical test. The hardening curve for sheet metal can be determined from the load–displacement curve of tensile specimen with rectangular cross-section. In this study, circle grids were imposed on the specimen surface to calculate true strains at different positions of the specimen. It is found that the load added to the different segments of specimen just before fracture can be determined by the maximum load and breaking load. True strains and corresponding true stresses can be determined after the specimen is pulled to fracture, so the hardening curve can be easily achieved. After a great deal of experiment, the results revealed that the tapered specimen had almost the same key parameters as the multi-stepped specimen, and the former is more easily used. Meanwhile, the work-hardening exponent (n) and the coefficient of normal anisotropy (r) can be obtained conveniently, and the forming limit line can also be approximately induced. The tapered and multi-stepped specimen with circle grids approach to determine the hardening curve were proposed and verified. The tapered specimen method was preferred for its simplicity in manufacturing .A tapered specimen with circle grids was similar to a multi-stepped specimen in view of the variable cross-section areas. In contrast to the three-stepped specimen, the major advantage was that the hardening curve can be directly obtained, which avoids the problem whether the hardening curve agrees with the power function or not.

Brun *et. al* [10] have analyzed incremental elastic deformations superimposed upon a given homogeneous strain with a boundary element technique. This is based on a recently-developed Green's function for non-linear incremental elastic deformations. Plane strain perturbations are considered of a broad class of incompressible material behaviours (including hyper-, hypoelastic and Navier–Stokes constitutive equations) within the elliptic range. Numerical treatment of the problem is detailed. A possibility of employing the method in the fully non-linear range is outlined, which yields a boundary element approach where the use of domain integrals is avoided, at least in a conventional sense.

Mielke [11] considered elasto-plastic deformations of a body which is subjected to a timedependent loading. The model includes fully nonlinear elasticity as well as the multiplicative split of the deformation gradient into an elastic part and a plastic part. Using the energetic formulation for this rate-independent process a time-incremental problem, which is a minimization problem with respect to the deformation and the plastic variables was derived. An assumptions on the constitutive laws of the material which guarantee that the incremental problem can be solved for as many time steps as desired was provided. The method relies on the polyconvexity of the so-called condensed energy functional and on a priori estimates for the plastic variables using the dissipation distance.

Tourabi *et. al* [12] performed biaxial tensile tests on cruciform specimens with the help of direct biaxial testing machine. Small offset-strain yield curves were detected on an aluminium alloy (AL1200) rolled sheet submitted to irreversible radial and complex biaxial tensile loadings. A predominant kinematic hardening and an important isotropic expansion were observed. A yield curve distortion was observed as well but, unlike the traction–torsion case, its intensity appears to be linked to the loading type. Moreover, the strain responses were analyzed in order to point out the pronounced anisotropy of the rolled sheet and to check if the sheet behavior was in agreement with a plastic flow associated with the yield curve. The experimental results obtained clearly revealed the interesting possibilities of the biaxial tensile test technique. The main objective of this study was to observe the distortion of the yield curves in the biaxial tensile plane. It was observed that the hardening along the equibiaxial loading respects, to some extent, the symmetry of the yield curves with regard to the loading path, with the existence of both a sharp front and blunt rear. On the other hand, contrary to the yield curves obtained in traction–torsion studies, the hardening observed along the tensile and corresponding complex loadings do not exhibit a significant distortion. Moreover, the application of different radial loadings enables to point out the influence of the loading type on the intricate appearance of anisotropy. In particular, the sheet symmetries influence deeply the orientation of the strain responses. The direct curves (tensile or mixed ones) and the corresponding transposed curves have different lengths, but similar orientations. Finally,

it was shown that the experimental results are in good agreement with a plastic flow associated to the yield criterion.

Cantemir *et. al* [13] presented a methodology for simulation of perforated plates multipass welding in order to compute residual stress and distortion, using FEM.Perforated plates were widely used as components in heat transfer equipment, playing a vital role in the plant safety. When their fabrication includes welding, the distortions due to this process should be estimated and reduced, as much as possible. The only way to do it in the design stage is by modeling and simulation, the most suitable method being the finite element method (FEM). It involved a combination of 2D and 3D analyses, thermo-elastic-plastic and elastic models, sub modeling, equivalent material data and experimental work. A new procedure for tube holes distortion assessment, in the case of large perforated plates fabricated by welding together two or more pieces, was proposed. It was based on finite element welding simulation and on some assumptions commonly employed in this field. Also, an important component was the experimentation, carried out in order to calibrate the numerical models. The procedure was versatile and could be used for many other applications involving perforated plates welding. However, for big variations of important parameters, like plate thickness for example, new experiments were strongly advised. The procedure results regarding tube holes distortion have been verified through an experiment. Good agreement between experimental measured and numerically computed data was found. Some other verifications are under way and, also, some new experiments for different welding processes and parameters, for different geometries and sizes.

Celentano *et. al* [14] have presented experimental and numerical analyses of the mechanical behaviour occurring in cylindrical and sheet specimens during the standard tensile test applied to SAE 1045 steel. A characterization of the material response using cylindrical specimens has been firstly performed in order to obtain the stress–strain curve and the diameter evolution at the neck which allow, in turn, to derive the elastic and hardening parameters by means of a well-established methodology. Then, a finite element large strain elastoplasticity-based formulation has been proposed and used to

simulate the tensile deformation process in such type of samples. Moreover, these material properties have been considered in the subsequent numerical analysis of the tensile test using sheet specimens. The results provided by both simulations have been satisfactorily validated with experimental data. In particular, the necking formation, which was found to be diffuse for both cases, has been properly described. Afterwards, a successful experimental hardening characterization carried out for sheet specimens using a correction factor deduced from the simulation has been performed. Finally, the proposed methodology has enabled to achieve an adequate description of the mechanical response of the material during the whole tensile test when using either cylindrical or sheet specimens.

Huetink *et. al* [15] described a new integration algorithm for large strain plastic deformations. The algorithm degenerates to the Euler forward elastoplastic-plastic model for small strain increments and to the rigid-plastic model for large strain increments. The model benefits from the advantages of both models: accuracy and fast convergence over a large range of strain increments.

Young *et. al* [16] performed a series of tests on cold-formed stainless steel square and rectangular hollow sections subjected to major axis bending. The tests were performed on sections fabricated by cold-rolling from normal strength material of austenitic stainless steel type 304, and high strength material of duplex and high strength austenitic steel sheets. The stainless steel type 304 was considered as normal strength material, whereas the HSA and duplex were considered as high strength material. Tensile coupon tests were conducted to obtain the material properties of the test specimens. The test strengths were compared with the design strengths obtained using the American Specification and Australian/New Zealand Standard for stainless steel structures. The North American Specification for cold-formed carbon steel structural members was also used to predict and compare the bending strengths. In addition, the test strengths were compared with the theoretical elastic and plastic bending moments. It is shown that the design strengths predicted by the three specifications and the theoretical bending moments were generally conservative for the tested specimens. The reliability analysis

was performed to evaluate the reliability of the design rules based on the existing resistance factors and load combination specified in the aforementioned specifications. It is shown that the American Specification and North American Specification were reliable for both normal and high strength specimens. The Australian/New Zealand Standard was reliable for normal strength specimens, but slightly unreliable for high strength specimens. The reliability of the design rules was evaluated using reliability analysis. It is demonstrated that the design strengths predicted by the ASCE Specification and NAS Specification were conservative and reliable for the normal and high strength stainless steel tubular sections. For the AS/NZS Standard, the design strengths were conservative and reliable for the normal Strength specimens when calibrated with the existing resistance factor of 0.9. The value of reliability index (βo) is slightly less than the target reliability index of 3.0 for the high strength specimens.

Simo and Taylor [17] have developed an unconditionally stable algorithm for plane stress elastoplasticity, based upon the notion of elastic predictor-return mapping (plastic corrector). Enforcement of the consistency condition is shown to reduce to the solution of a simple nonlinear equation. Consistent elastoplastic tangent moduli are obtained by exact linearization of the algorithm. Use of these moduli is essential in order to preserve the asymptotic rate of quadratic convergence of Newton methods. The accuracy of the algorithm is assessed by means of iso-error maps. The excellent performance of the algorithm for large time steps is illustrated in numerical experiments.

Simandjuntak *et. al* [18] have examined the effect of plasticity induced crack closure on fatigue crack growth rate for the case of a 2024 aluminium alloy plate with two lateral corner cracks emanating from a central hole. A three-dimensional finite element quarter model was developed of the plate with a central hole and corner cracks. The load on the model was cycled and the crack extended by releasing nodes so as to predict the development of a plastic wake behind the advancing crack. The opening load was predicted from the finite element displacement versus load results. These opening load predictions agreed favourably with the experimental measurements. The finite element model was also used to predict the fatigue crack growth rate. This was achieved

by first evaluating the effective stress intensity factor range from the stress distribution ahead of the crack tip. Encouraging comparisons of the finite element predictions of fatigue crack growth rate with experimental measurement were obtained.

Sander *et. al* [19] have presented a detailed elastic–plastic finite element analysis of the fatigue crack growth after mixed mode overloads in order to understand the mechanism of the load interaction effects. By such numerical simulations, it can be shown that, due to mixed mode overloads, plastic deformations occur, which on the one hand reduce the near-tip closure and on the other hand cause a far-field closure. Also the stress distribution before and after the crack tip changes. A mixed mode overload causes lower closure and the crack tip deformations become asymmetrical, which is a reason for the smaller retardation effect of a mixed mode overload.

Bernasconi *et. al* [20] have presented the results of an experimental investigation of the multiaxial fatigue behaviour of the R7T steel. The R7T steel is currently employed in the production of solid high-speed railway wheels. Wheel failures due to rolling contact fatigue may occur and, on some occasions, fatigue cracks nucleate in the sub-surface region under the contact area between wheel and rail. Here, the stress field is multiaxial and the loading path is non-proportional. Specimens extracted from the rim of railway wheels were subjected to combined out-of-phase alternating torsion and pulsating compressive axial loads, a non-proportional stress state which is similar to that observed under the contact area in the wheel rim. The tests results are discussed in the light of some multiaxial fatigue theories, chosen among those based on the critical plane concept and those implementing an integral approach, with the aim of selecting a fatigue criterion suitable for the sub-surface fatigue assessment of railway wheels.

Unosson *et. al* [21] have proposed a method to better handle fracture using element erosion in finite element analyses is proposed. It is assumed that the crack-tip is blunt and that the solution in the vicinity of the crack-tip is separable when described in local polar co-ordinates. The numerical solution is enhanced by scaling strain rates at

integration points to better match the state at the crack-tip. This material specific scaling function is empirically determined for modus I steady-state propagation and is applied to two problems. The results show that the method reduces mesh dependency such that the chosen fracture energy can be better matched for different element sizes.

2.2 SUMMARY OF LITERATURE REVIEW

From the literature review discussed above, it is seen that FEM is used as a tool for various types of elasto-plastic analysis of different components in different loading conditions using the material required. Earlier the design of the component was based on experimental data and manual calculations which was a time consuming and yield lesser degree of safety and optimization of the component. FEM is useful in reducing all these problems. By using FEM analysis technique simulation of the real geometry and boundary conditions can be done with loading conditions accurately. The results can be visualized in terms of stresses, strain and deflections as a response of loading.

CHAPTER 3

ANALYSIS

3.1 INTRODUCTION

Tensile test is a useful engineering procedure to calculate elastic and plastic variables related to mechanical behaviour of tools. It is recognized that changes in the geometry of the part plays an important role in the material response during the actual loading conditions. In the present work the tensile test on the material used in the railway coaches namely *Corten Steel* is done. This material is used to make the *underframe* of railway coach .There after, the FEM analysis of the component is done. Finite Element Method has become a powerful tool for the numerical solution of a wide range of engineering problems.

In the following section the formulation of elasto-plastic analysis problem is discussed.The work is divided into three parts. First part deals with the experimental procedure, second part deals with Finite Element analysis and third part with the experimental characterization and numerical simulation.

3.2 EXPERIMENTAL PROCEDURE

The experimental procedure which is adopted in the present work consists of following steps:

1. The material i.e. *Corten Steel* is cut into sheet specimens. Specifications are shown in fig 3.1.

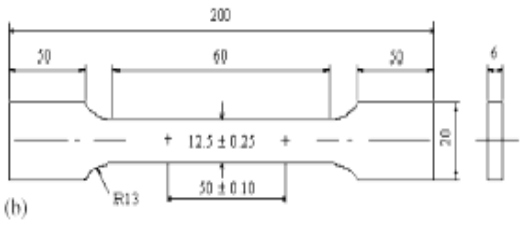

Fig 3.1. Geometric configuration for sheet sample.

2. Chemical characterization to check an adequate composition was done.
3. Mechanical Tensile test was done. The engineering stress-strain curve using sheet specimens considering a load cell speed of 2.5 mm/min are plotted. The engineering stress is computed as P/A_0, where P is the axial load and A_0 is the initial transversal area. The engineering strain or elongation is computed as $(L - L_0)/L_0$, with L and L_0 being the current and initial extensometer lengths, respectively.
4. Characterization of the plastic behaviour. At high levels of elongation, the stress and strain distributions are no longer uniform along the specimen due to the necking formation that takes place for sheet samples. Therefore, the stress–strain curve obtain after tensile test cannot provide a proper description of the physical phenomena involved in the test. So , the mechanical response can be adequately described by an alternative stress–strain curve defined in terms of the mean equivalent stress $\bar{\sigma}_{eq}$ versus an equivalent deformation ε_{eq} (composed of an elastic and plastic contributions) respectively given by $\bar{\sigma}_{eq} = f_B P/A$ and $\varepsilon_{eq} = \bar{\sigma}_{eq}$ /E+ ε_p, where $f_B(\varepsilon_p) \leq 1$ is an assumed known correction factor applied to the mean true axial stress P/A, A is the current transversal area at the necking zone ($A = wt$ for the sheet samples, where w and t are the current width and thickness of the neck), E is the Young's modulus and $\varepsilon_p = \ln(A_0/A)$ is the true (logarithmic) deformation.

3.3 FINITE ELEMENT ANALYSIS

Consider the uniaxial stress-strain curve shown in fig 3.2. The behaviour is initially linear elastic with slope E (young's modulus) until onset of yielding at the uniaxial yield stress, σ_Y. Thereafter, the material response is elasto-plastic with the load tangent to the curve, E_T, called the elasto-plastic tangent modulus, continually changing.

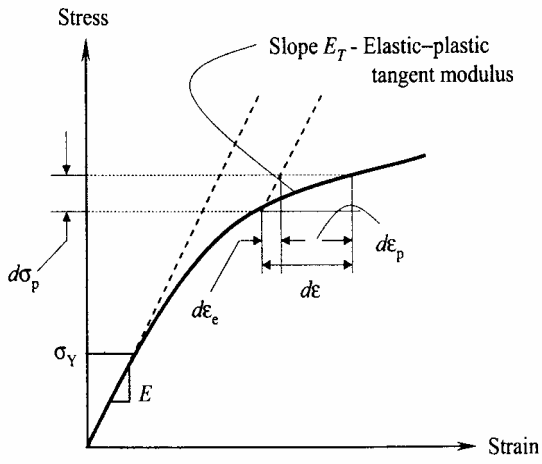

Fig 3.2. A strain hardening plastic behaviour for the uniaxial case.

At some stress level σ in the plastic range, if the load is increased to induce a stress of $d\sigma$, it results in a corresponding strain $d\varepsilon$. This increment of strain contains two parts: elastic $d\varepsilon^e$ (recoverable) and plastic $d\varepsilon^p$ (non-recoverable):

$$d\varepsilon = d\varepsilon^e + d\varepsilon^p, d\varepsilon^e = \frac{d\sigma}{E}, \frac{d\sigma}{d\varepsilon} = E_T \tag{3.1}$$

The strain hardening parameter, H, is defined by

$$H = \frac{d\sigma}{d\varepsilon^p} = \frac{\dfrac{d\sigma}{d\varepsilon}}{1 - \dfrac{d\varepsilon^e}{de}} = \frac{E_T}{1 - \dfrac{E_T}{E}} \tag{3.2}$$

The element stiffness for the linear elastic portion is:

$$\left[K^e\right] = \int_{x_a}^{x_b} \left[B\right]^T \left[D^e\right] \left[B\right] dx \tag{3.3}$$

where $\left[D^e\right]$is the linear elasticity matrix(D^e=E for the uniaxial case).when the element deforms plastically, $\left[D^e\right]$ reflects the decreased stiffness. This is computed, for uniaxial material behavior, by the following procedure: the increment in load dF causes an increment displacement du

$$du = h_e d\varepsilon_{xx} = h_e\left(d\varepsilon^e + d\varepsilon^p\right), dF = Ad\sigma = A_e H d\varepsilon^p \tag{3.4}$$

where h_e is the length and A_e the area of cross-sectional of the element. The effective stiffness is

$$E^{ep} = \frac{dF}{du} = \frac{A_e H d\varepsilon^p}{h_e\left(d\varepsilon^e + d\varepsilon^p\right)} = \frac{EA_e}{h_e}\left[1 - \frac{E}{\left(E+H\right)}\right] \tag{3.5}$$

The element stiffness for plastic range becomes,

$$\left[K^{ep}\right] = \int_{x_a}^{x_b} \left[B\right]^T \left[D^{ep}\right] \left[B\right] dx \tag{3.6}$$

where $\left[D^{ep}\right]$ is the material stiffness in the plastic range. For uniaxial case $D^{ep} = E^{ep}$. Eq(3.3) is valid when $\sigma < \sigma_Y$ and eq(3.6) is valid for $\sigma > \sigma_Y$. $d\sigma = \sigma - \sigma_Y$ when $\sigma > \sigma_Y$.

3.3.1 ELASTIC-PLASTIC ANALYSIS

In this section a detailed computational procedure for the analysis of an elasto-plastic problem is presented. The procedure is described via a one-dimensional elasto-plastic bar problem. A linear strain-hardening material subjected to an increasing uniaxial load is conidered.

- **UPDATE OF STRESSES**

At a load-step number r where the deformation is elastic, the stress in a typical element with the strain increment $\Delta\varepsilon^r$ can be readily updated as

$$\sigma_i^r = \sigma_i^{(r-1)} + E_i \Delta\varepsilon^r \tag{3.7}$$

where E_i is the elastic modulus of element *i*. This linear elastic behavior will continue up till a point where the resulting strain increment will initiate plastic yielding of the material. Now the updating of the stress in the element is not as straightforward as given in eq.(3.7), and it can get complicated when the deformation is partly elastic and partly elasto-plastic ,as shown from point *A* to *B* in the stress-strain curve of fig.3.3

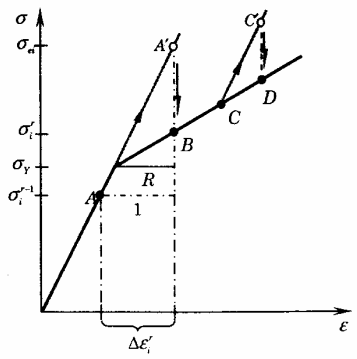

Fig 3.3 Transition of elastic to elasto-plastic behaviour

To update the stress state from point *A* to *B*, one can first assume that the deformation is elastic and compute the corresponding elastic stress, commonly referred to as the elastic predictor .Using eq.(3.7),the elastic stress predictor σ_e can be calculated as

$$\sigma_{ei} = \sigma_i^{(r-1)} + E_i \Delta\varepsilon_i^r \tag{3.8}$$

Computing the elastic stress predictor brings the stress state from point *A* to *A′* .A correction is made to transfer the stress state back to the elasto-plastic state at point *B*. A correction factor *R* is introduced.

$$R = \frac{\sigma_{ei} - \sigma_y}{\sigma_{ei} - \sigma_i^{(r-1)}} \tag{3.9}$$

so that the stress at point *B* can be written as

$$\sigma_i^r = \sigma_i^{(r-1)} + \left[(1-R)E_i + RE_T\right]\Delta\varepsilon_i^r \tag{3.10}$$

here E_T denotes the elastic-plastic tangent modulus, which is related to the elastic modulus *E* and strain hardening parameter *H* by eq.(3.2). In the case where the element has already yielded in previous load steps, as illustrated by point *C* in fig.3.3 ,the approach of determining the elastic stress predictor and making correction to the stress state at point *D* still applies *R*=1 in eq(3.10).

$$\sigma_i^r = \sigma_i^{(r-1)} + E_T \Delta\varepsilon_i^r \tag{3.11}$$

- **UPDATE OF PLASTIC STRAIN**

The extent of plastic flow in a deformed material can be readily characterized by the measure of plastic strain. To determine the plastic strain in an element at point B of fig.3.3, it will be useful to rewrite eq. (3.10) as

$$\sigma_i^r = \sigma_Y + E_T\left(R\Delta\varepsilon_i^r\right) \equiv \sigma_Y + \Delta\sigma_i^r \tag{3.12}$$

Eq (3.12) can be interpreted as that adjusts the stress state at point A to the yield stress before predicting the elastic stress and its correction. This will allow one to isolate the stress component $\Delta\sigma_i^r$ and strain $R\varepsilon_i^r$ that are involved in the plastic flow. With eq(3.1), the plastic strain increment is

$$\Delta\varepsilon_{pi}^r = R\Delta\varepsilon_i^r - \frac{\Delta\sigma_i^r}{E_i} = \left(1 - \frac{E_T}{E_i}\right)R\Delta\varepsilon_i^r \tag{3.13}$$

Eq (3.13) can also be used for elements that have already yielded in previous load steps by setting R=1.

- **UPDATE OF YIELD STRESS LIMIT**

Besides assessing the extent of plastic deformation, the measure of the plastic strain will become especially crucial for strain-hardening materials where the yield limit is a function of the plastic strain. A plot of yield limit against the plastic strain for a typical linear strain-hardening material is shown in fig 3.4. Once the plastic strain occurs, the yield limit will be modified and updated as

$$\sigma_{yi}^r = \sigma_Y + H\Delta\varepsilon_{pi}^r \tag{3.14}$$

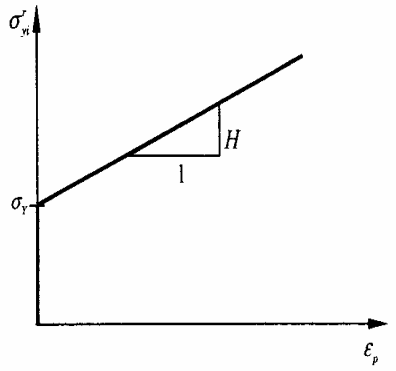

Fig 3.4 Stress-strain behaviour of a strain hardening material

- **IDENTIFICATION OF DEFORMATION MODES**

The updated yield limit will come in handy when one is to check the type of deformation an element is undergoing. Once the correct type of deformation is identified, the stress and strain values can then be updated according to eq (3.10) and (3.13).there are four types of deformation.

(a) Elastic Loading: (an element that has not yielded previously continues to deform elastically)

$$\left|\sigma_i^{r-1}\right| < \left|\sigma_{yi}^{r-1}\right| \text{ and } \left|\sigma_{ei}\right| < \left|\sigma_{yi}^{r-1}\right| \qquad (3.15a)$$

(b) Elastic-Plastic Loading: (an element that has not yielded previously will deform elasto-plastically)

$$\left|\sigma_i^{r-1}\right| < \left|\sigma_{yi}^{r-1}\right| \text{ and } \left|\sigma_{ei}\right| > \left|\sigma_{yi}^{r-1}\right| \qquad (3.15b)$$

(c) Plastic Loading: (an element that previously yielded will continue to deform plastically)

$$\left|\sigma_i^{r-1}\right| > \left|\sigma_{yi}^{r-1}\right| \text{ and } \left|\sigma_{ei}\right| > \left|\sigma_i^{r-1}\right| \qquad (3.15c)$$

(d) Elastic Unloading: (an element previously yielded is now unloading elastically)

$$\left|\sigma_i^{r-1}\right| > \left|\sigma_{yi}^{r-1}\right| \text{ and } \left|\sigma_{ei}\right| < \left|\sigma_i^{r-1}\right| \qquad (3.15d)$$

- **FORCE EQUILIBRIUM**

Since the displacement finite element model is based on the principle of virtual displacements, the solution satisfies the equilibrium equations, provided the deformation is linearly elastic. However, in the finite element analysis of elasto-plastic problems equilibrium equations may not be satisfied during the period when stresses are adjusted to account for plastic strains. Adjustments must be made to achieve equilibrium at each step by redistributing the forces neighboring elements.

For example, consider a node N at the interface of element *i* that has yielded and the adjacent element i+1 that is still elastic (fig 3.5). At this node, the force equilibrium will be violated during the analysis because the force in element *i* is limited such that the stress in the element does not exceed the yield stress. The difference between the force

calculated using the elastic analysis and the plastic force must now be taken up by all other elastic elements in the mesh. Thus to restore equilibrium of forces, a force correction must be made at the node N:

$$\Delta F = F_i - F_{i+1} - F_N \tag{3.16}$$

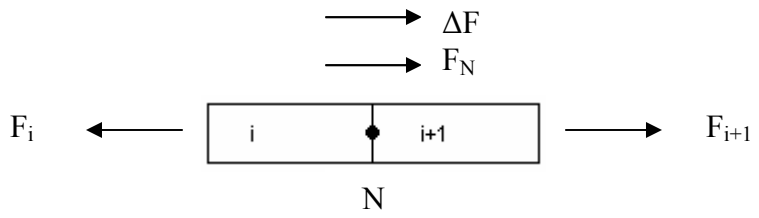

Fig 3.5 Force equilibrium at node N

However, to preserve the Finite element equations of the original problem (to retain the same forces in other unaffected elements), the force correction cannot be imposed as a nodal force. Instead, the force correction may be applied as a nodal displacement

$$\Delta u_N^c = \frac{\Delta F L_i}{E_T A_i} \tag{3.17}$$

where L_i and A_i are the length and cross-sectional area of element i. This correction procedure will continue until force equilibrium at all nodes is restored, within an acceptable error of tolerance.

3.4 EXPERIMENTAL CHARACTERIZATION AND NUMERICAL SIMULATION

The main objective of the present analysis is to validate the predictions of the above formulation with the experimental data obtained in the tensile tests of C*orten Steel* in order to achieve an adequate mechanical characterization of this material when sheet specimens are considered. Numerical simulation is done using C++ source code. Using this program the experimental and numerical analysis of tensile test using sheet specimens is tested, implemented and verified.

3.5 ALGORITHM OF THE PROGRAM

The following steps are followed for the development of the program for elasto-plastic analysis of the sheet specimens.

1. Allocate memory for the required matrix.
    - Input the initial dimensions of the sheet specimen and initial connectivity.
    - Initialize the load matrix and increment it in each new step.
    - Input the force matrix.
    - Calculate the total no. of joints, total no. of elements for the specimen according to the number of divisions entered by the user.
    - x [total no. of joints] for the coordinate of the sheet specimen.
    - Connectivity matrix given by connect [total no. of elements] [no. of nodes/element], which gives the connectivity between different elements.
    - Element stiffness matrix given by estiff [total no. of nodes/element x dof] [total no. of nodes/element x dof].
    - System stiffness matrix given by a [total no. of joints x dof] [total no. of joints x dof].
    - Boundary condition matrix, given by bcc [total no. of joints x dof].
    - Load matrix, given by b [total no. of joints x dof].
2. Mesh is generated using one dimensional element as shown in fig 3.6.

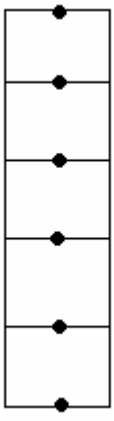

Fig 3.6 Mesh generation in x direction

3. Starting from the first element, find the element stiffness matrix for each element.
4. Assemble all the element stiffness matrices into a system stiffness matrix.
5. Now modify the system matrix according to the boundary conditions.
6. Matrix is solved using the solver (Gauss Elimination Method is used in this case).
7. This will give the value of the displacement, for all the nodes of the specimen.
8. Now the value of stress is calculated.
9. Then calculate the strain increment for each element.
10. Calculate the Element elastic stress predictor and yield stress limit using eq.3.8 and eq.3.14 respectively.
11. Compute whether element has yielded in the previous load step or not by using eq.3.15c.
    - If yes, then compute whether element is unloading elastically or continues to yield.
        - If yes, then put correction factor,*R* to 0 and go to step 12.
        - Otherwise, put *R*=1 and shift to element stiffness matrix for plastic range in next load step and go to step 12.
    - Otherwise, compute whether element is deforming elastically or has just yielded.
        - If yes, then put *R*=0 and go to step 12.
        - Otherwise, put $R = \frac{\sigma_{ei} - \sigma_y}{\sigma_{ei} - \sigma_i^{(r-1)}}$ and shift to element stiffness matrix for plastic range in next load step and go to step 12.
12. Update element stress and plastic strain using eq.3.10 and eq.3.13.
13. Now, check whether equilibrium is satisfied at each node or not using eq 3.16
    - If yes, then go to the next load step and repeat from step 1 to 15 until equilibrium is satisfied and last load step is reached.
    - Otherwise, modify nodal displacements using eq.3.17 and go to step 12 and repeat up to 15 until equilibrium is satisfied and last load step is reached.

Fig 3.7 shows the flow chart for the elasto-plastic analysis.

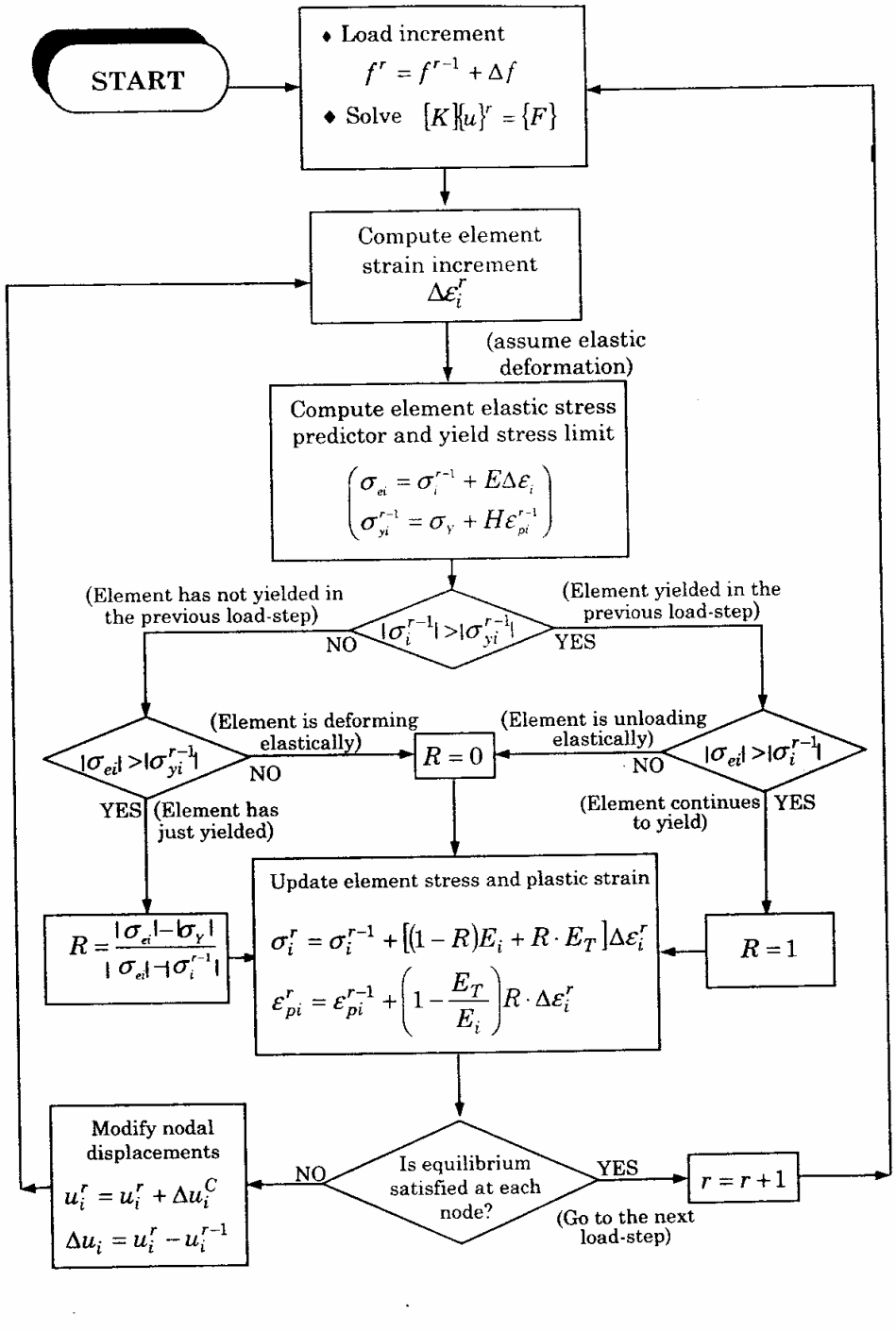

Fig 3.7 Flow chart for elasto-plastic analysis

CHAPTER 4

RESULTS AND DISCUSSION

4.1 INTRODUCTION

An experimental analysis and a numerical simulation of the mechanical behaviour occurring in sheet specimens during the standard tensile test have been done. The study has been focused on the Corten Steel material for which the classical procedure to predict the stress distribution at the neck cannot be used directly.

Applying experimental-numerical methodology, an experimental characterization of the material response has been performed in the present work in order to obtain a proper stress-strain curve, which allows us, in turn to derive the elastic and hardening parameters for this material. Then, a finite element based elasto-plastic formulation has been proposed and used to simulate the whole tensile deformation process. The results provided by the simulation have been successfully validated with the D.J.Celentano *et.al* [14]. The plastic evolution that takes place before and after the necking formation has been described properly. The technique of finite element has been applied to the analysis of the tensile test of sheet specimen and is versatile in that it allows the model established to be easily changed, enabling a thorough examination of the effect of loading.

The sheet specimens are analyzed experimentally and numerically simulated for finding out the behaviour of the material. The specimens used are shown in fig 4.1.

Fig 4.1 Corten Steel sheet specimen

4.2 RESULTS VALIDATION AND DISCUSSION

- The chemical characterization was done to check the adequate amount of composition of Corten Steel. This is carried out by means of an optical spectrometer. The average chemical composition for the studied material is shown in table 1.

Table1. Analysis of Corten Steel tension specimen: average chemical composition (%)

C <0.10	Mn 0.25-0.45	Si 0.28-0.72	Ni 0.20-0.47	Cu 0.30-0.60
Cr 0.35-0.60	S <0.03	P 0.075-0.140	Mo <0.05	V <0.05
Al <0.08	Nb <0.04	Fe 98.2		

- The mechanical tensile test was conducted. The average engineering stress strain curve obtained considering a load cell speed of 2.5 mm/min is plotted in fig 4.2.

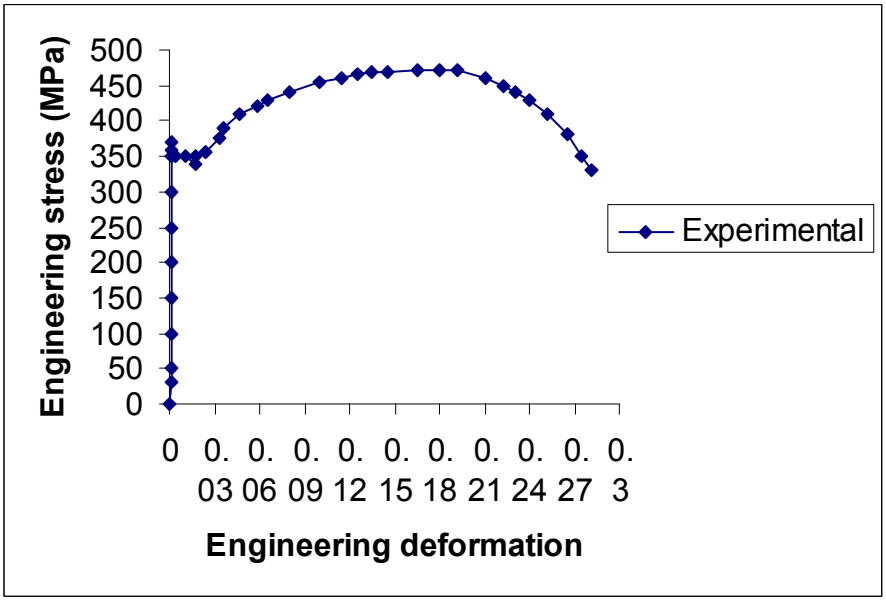

Fig 4.2 Analysis of sheet specimen: experimental values of average stress-strain curve

At the beginning of the deformation process, the material behaves elastically. After the yield strength is reached, the plastic hardening begins and the load increases up to a maximum value of specified elongation. Then the load decreases since the effect of the reduction of the transversal area at the necking zone is stronger than that of the hardening mechanism.

The average experimentally measured values for the maximum load, maximum engineering stress, elongation at fracture stage, young's modulus and yield strength are summarized in table 2 and 3.

Table 2. Analysis of the tensile test: average experimentally measured values.

Material/sample	Maximum load (KN)	Maximum engineering stress (MPa)	Elongation at the Fracture stage (%)
Corten Steel/Sheet	33.9	470.9	28.4

Table 3. Analysis of tensile test: material properties considered in the numerical simulation

Material Properties	Corten Steel
Young's modulus	200800 MPa
Poisson's ratio	0.30
Yield strength	350 MPa

- After this the characterization of the plastic behaviour was done. At high level of elongation, the stress strain distributions are no longer uniform along the specimen due to the necking formation that takes place for sheet specimens. Therefore, the stress–strain curve obtain after tensile test cannot provide a proper description of the physical phenomena involved in the test. So , the mechanical response can be adequately described by an alternative stress–strain curve defined

in terms of the mean equivalent stress $\bar{\sigma}_{eq}$ versus an equivalent deformation ε_{eq} (composed of an elastic and plastic contributions) respectively given by $\bar{\sigma}_{eq} = f_B P / A$ and $\varepsilon_{eq} = \bar{\sigma}_{eq}/E + \varepsilon_p$, where $f_B(\varepsilon_p) \le 1$ is an assumed known correction factor applied to the mean true axial stress P/A, A is the current transversal area at the necking zone ($A = wt$ for the sheet samples, where w and t are the current width and thickness of the neck), E is the Young's modulus and $\varepsilon_p = \ln(A_0/A)$ is the true (logarithmic) deformation. Using specimens of the material, the experimental values for the P - ε_p and P/A - ε_p are preliminarily plotted in fig 4.3 (a)-(c).

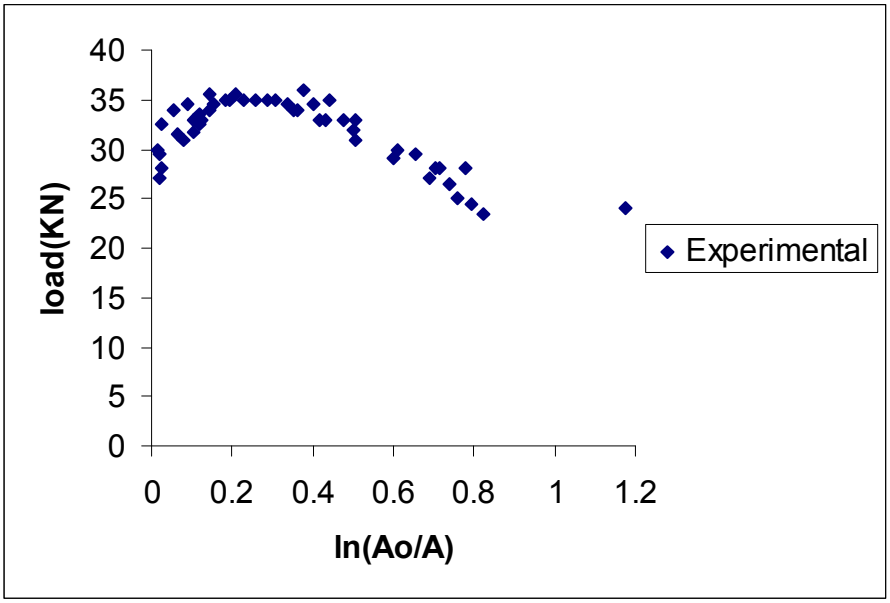

Fig 4.3. (a) Analysis of the sheet specimen: load versus true deformation

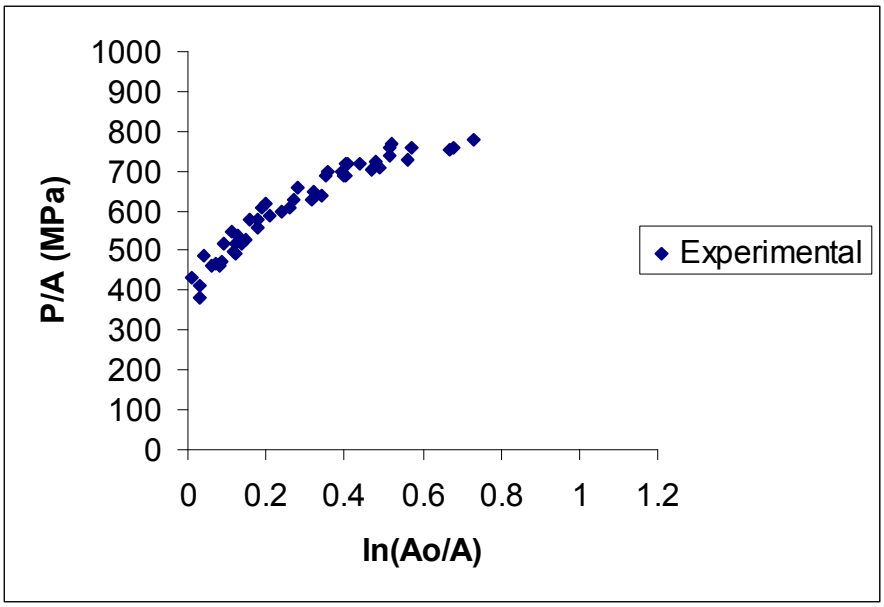

Fig 4.3. (b) Analysis of the sheet specimen: mean true axial stress versus true deformation

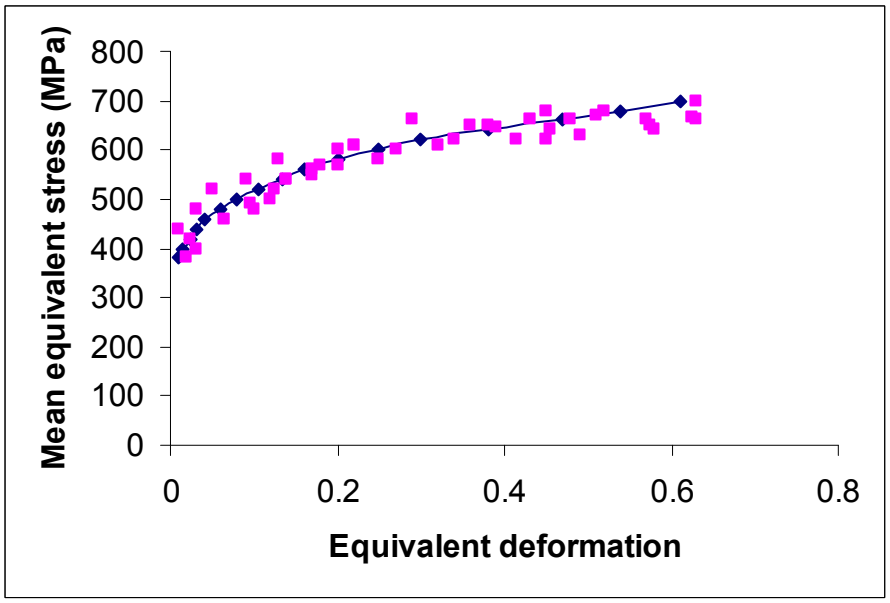

Fig 4.3. (c) Analysis of sheet specimen: mean equivalent stress versus equivalent deformation

The correction factor to be applied for this case depends not only on the type of the samples used but also on the strain, ε_p^* which is the maximum logarithmic deformation at which the strain and strain distribution are normal along the specimen. Table 4 summarizes the correction factor as a function of the true deformation related to the sheet sample with ε_p^*=0.10 ($f_B = 1$ for $0 \le \varepsilon_p \le \varepsilon_p^*$ where ε_p^* is a material characteristic parameter).

Table 4. Analysis of the test: correction factor as a function of true deformation

$\ln(A_0 / A)$	Sheet sample correction factor ε_p^*=0.10
0.00	1.000
0.05	1.000
0.10	1.000
0.20	0.976
0.30	0.955
0.40	0.933
0.50	0.909
0.60	0.884
0.70	0.858
0.80	0.830
0.90	0.800
1.00	0.769

In the present analysis, the adequate experimental data for the $\overline{\sigma}_{eq} - \varepsilon_{eq}$ relationship have been achieved by using the correction factor associated with sheet specimen. Fig 4.4 shows the geometric configuration of broken specimens at the end of the test for the material studied, conforming, the development of diffuse necking.

Fig 4.4 Analysis of tension specimen: fracture stage for Corten steel (sheet sample)

- FINITE ELEMENT ANALYSIS

The finite element mesh as shown in fig 3.6 of sec.3.5 and methodology is used in order to describe correctly the large stress and deformation expected in the necking zone. The sheet specimen is discretized with a one-dimensional finite element mesh with a height of 50mm (initial extensometer length).

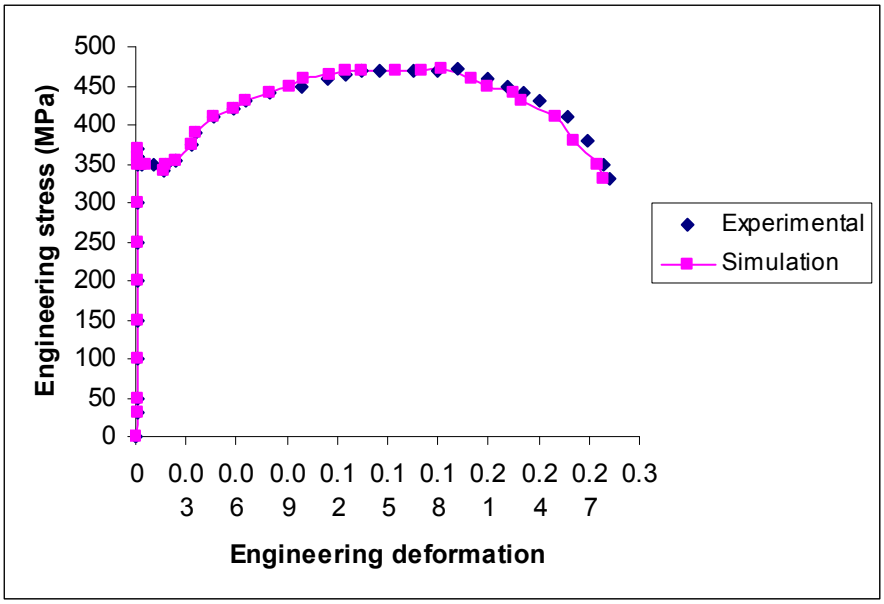

Figure 4.5 Analysis of sheet specimen: engineering stress strain relationship

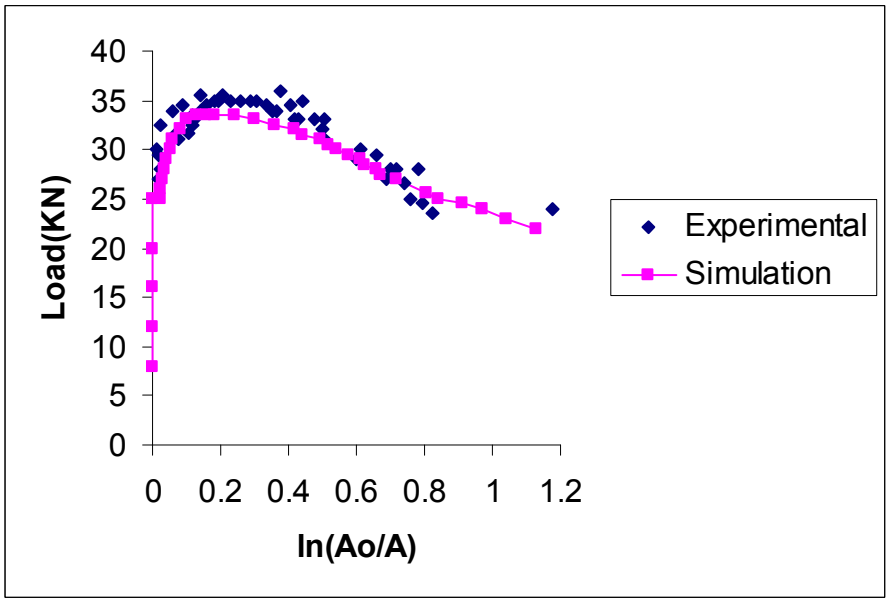

Fig 4.6 (a) Analysis of sheet specimen, results at the section under going extreme necking: load versus true deformation

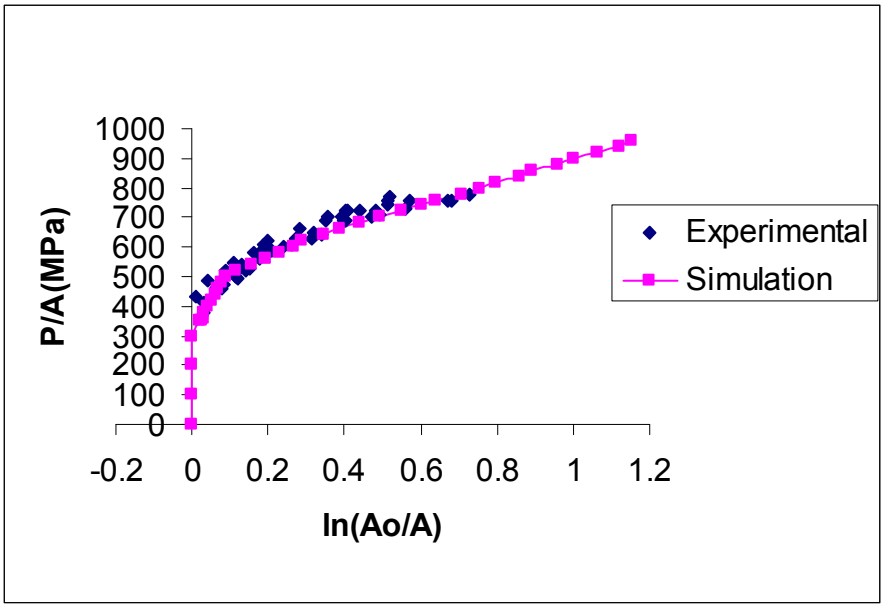

Fig 4.6. (b) Analysis of sheet specimen, results at the section under going extreme necking: mean true axial stress versus true deformation

Fig 4.5 shows the engineering stress-strain relationship and fig 4.6 (a)-(b) shows some results at the section undergoing extreme necking (average width and thickness ratios versus the elongation and the load and mean true axial stress, both against the logarithmic deformation). In this case the results provided by simulation properly adjust the average experimental data. The discrepancies appearing in these curves can be considered, in general, approximately bounded with the experimental uncertainty range.

The necking formation promotes a geometrical instability that develops until the fracture of the specimen. The respective engineering and logarithmic strains at the point of the maximum load are 17.6% and 0.205 for the experiments and 17.3% and 0.200 for the numerical simulation. The plastic evolution occurring before the necking formation (both the nearly perfectly plastic part and the zone with significant hardening) is well captured by the simulation.

CHAPTER 5

CONCLUSION

This chapter gives the conclusions as obtained from the results of the analysis of the tensile test using sheet specimens of Corten Steel using finite element based elasto-plastic technique.

5.1 CONCLUSION

- While talking about transportation whether automobile, rail or plane the first word which comes to our mind is accident. Accidents are now a days an increasing fever which takes our mind out, even when thinking of them once. Accidents accounts for no. of reasons starting from technical to human mistakes. Human mistakes are unavoidable but the technical failures can be checked and the problems can be rectified. If we take the cases of rail then now a day's no. of accidents are happening here and many precious lives are lost. Taking into account this, the concept of crashworthy coaches came into existence. This demands, the collapse of end portion of the vehicle by permanent deformation and to avoid deformation of other/central part. For this, the behaviour of plastic deformation of the material is necessary to be known. So, these results are required to study the crashworthy behaviour of the structure.
- The study focused on the material reveals that the classical procedure to predict the stress distribution at the neck cannot be used directly and it does not provide any information about the mechanical behaviour of material in plastic range.
- The engineering stress-strain relationship and the results at the section undergoing extreme necking shows that the results provided by the simulation have been successfully validated with experimental data.

- The results also show that the plastic evolution that takes place before and after the necking formation has been described properly.

5.2 FUTURE SCOPE.

- The applicability of the proposed technique is restricted to isotropic material responses, its extension to anisotropic materials may also be possible by among different possibilities, including anisotropic effect in the yield criterion and plastic flow rule.
- The present finite element based elasto-plastic formulation is done using 1D mesh, this work can be extended using 2D and 3D mesh for different geometrical specimens.

BIBLIOGRAPHY

[1] George E. Dieter, *Mechanical Metallurgy-SI Metric Edition*, McGraw-Hill book Company, London, 1988.

[2] G.H.Ryder, *Strength of Materials*, B.I.Publications, India, 1964.

[3] O.C.Zienkiewicz, *The Finite Element Method*, Tata McGraw-Hill Publication, London, 1979.

[4] J. N. Reddy, *Finite Element Method*, McGraw-Hill International Editions, 1993.

[5] R. Tirupathi Chandrupatla and D. Ashok Belegundu, *Introduction to Finite Elements in Engineering*, Pearson Education, Singapore, 2004.

[6] M. James Gere and P Stephen Timoshenko, *Mechanics of Materials*, CBS Publishers and Distributors, 2002.

[7] S. Rajesekaran, *Finite Element Analysis in Engineering Design*, Wheeler Publishing, 1994.

[8] J.N.Reddy, *An Introduction to Nonlinear Finite Element Analysis,* OXFORD University Press, 2004.

[9] W.Johnson and P.B.Mellor, *Plasticity For Mechanical Engineers*,D.Van Nostrand Company Ltd.,1962.

[10] N.Eric.Simons, *Mechanical Testing of Metallic Materials*, Pitman.

REFERENCES

[1] Simo,J.C. and Armero,F.,"*Geometrically Nonlinear Enhanced Strain Mixed Methods and the Method of Incompatible Modes"* International Journal for Numerical Methods in Engineering,Vol.33,pp.1413-1449,1992.

[2] Morestin, F., and Boivin, M.," *On the Necessity of Taking into Account the Variation in the Young Modulus with Plastic Strain in Elastic-Plastic Software*",Nuclear Engineering and Design ,Vol.162.pp.107- 116,1996.

[3] Ling,Y.,"*Uniaxial True Stress-Strain after Necking*", AMP Journal of Technology, Vol. 5 , 1996.

[4] Albertini,C., Micunovic,M. and Montagnani,M.," *High Strain Rate Viscoplasticity Of AISI 316 H Stainless Steel From Tension And Shear Experiments*",1997.

[5] Mariani,S.,Corigliano,A. and Orsatti,B**.,"** *Identification of Gurson–Tvergaard Material Model Parameters via Kalman Filtering Technique. I. Theory*",International Journal of Fracture,Vol.104,pp.349-373,2000.

[6] Celentano,D.J.,"*A Large Strain Thermovicsoplastic Formulation for the Solidification of S.G.Cast iron in a green sand mould*",International journal of Plasticity,Vol.17,pp.1623-1658,2001.

[7] Govaert, L.E., Goijaerts, A.M., and Baaijens, F.P.T.,"*Experimental and Numerical Investigation on the Influence of Process Speed on the Blanking Process*", ASME Journal of Manufacturing Science and Engineering, Vol.124, pp.416-419, 2002.

[8] Gozzi, J., Olsson, A.," *Stainless Steel – Plasticity and Constitutive Modelling",* 2003.

[9] Kang, D., and Tian, H.," *A Study on Determining Hardening Curve for Sheet Metal"*,International Journal of Machine Tools & Manufacture,Vol.43,pp.1253–1257,2003

[10] Brun,M., Capuani,D. and Bigoni,D.," A boundary element technique for incremental,non-linear elasticity",Comutational Methods in Applied Mechanical Engineering,Vol.192,pp.2461-2479,2003.

[11] Milke, A.,"Existence of minimizers in incremental elasto-plasticity with finite strains"2003.

[12] Tourabi, A., and Losilla, G.," *Hardening of a Rolled Sheet Submitted to Radial and Complex Biaxial Tensile Loadings"*,International Journal of Plasticity,Vol.20,pp. 1789-1816, 2004.

[13] Cantemir, D., Bertini, L., and Beghini, M.,"*Finite Element Modeling and Simulation of Multi-Pass Welding for the Perforated Plates Case",* International Conference on Computational mechanics, 2004.

[14] Celentano, D.J.,"*Experimental and Numerical Analysis of the Tensile Test using Sheet Specimens*", Finite Element in Analysis and Design,Vol 40,pp.555-575,2004.

[15] Hunetink,J.,Van Den Boogaard,A.H., Rietman,A.D.,Lof,J. and Meinders,T.," *A Mixed Elastoplastic / Rigid-Plastic Material Model",*2004.

[16] Young, B., and Zhou, F.,"*Tests of Cold-formed Stainless steel Tubular Flexural Members*", Thin-Walled structures, Vol.43, pp.1325-1337, 2005.

[17] Simo,J.C. and Taylor, R.L," *A return mapping algorithm for plane stress elastoplasticity*", International Journal of Numerical Methods in Engineering,Vol.22, Issue.3, pp.649-670,2005.

[18] Simandjuntak,S., Alizadeh,H., Smith,D.J.and Pavier,M.J., "*Three dimensional finite element prediction of crack closure and fatigue crack growth rate for a corner crack",*International Journal of Fatigue,Vol 28,pp.335-345,2006.

[19] Sander,M. and Richard,H.A.," *Experimental and Numerical Investigations on the Influence of the Loading Direction on the Fatigue Crack Growth*", International Journal of Fatigue,Vol 28,pp.583-591,2006.

[20] Bernasconi,A., Filippini,M., Foletti, S. and Vaudo D.," *Multiaxial Fatigue of a Railway Wheel Steel under Non-proportional Loading*",International Journal of Fatigue,Vol.28,pp.663-672,2006.

[21] Unosson,M., Olovsson,L., and Simonsson, K.," Failure Modelling in Finite Element Analyses: Element Erosion with Crack-tip Enhancement", Finite Element in Analysis and Design, Vol 42, pp.283-297,2006.